Hindawi
Complexity
Volume 2017, Article ID 4324879, 8 pages
https://doi.org/10.1155/2017/4324879

Research Article

Stabilization of a Network of the FitzHugh–Nagumo Oscillators by Means of a Single Capacitor Based RC Filter Feedback Technique

Elena Adomaitienė,[1] Skaidra Bumelienė,[1] Gytis Mykolaitis,[1,2] and Arūnas Tamaševičius[1]

[1] *Department of Electronics, Center for Physical Sciences and Technology, Saulėtekio Av. 3, LT-10257 Vilnius, Lithuania*
[2] *Department of Physics, Vilnius Gediminas Technical University, Saulėtekio Av. 11, LT-10223 Vilnius, Lithuania*

Correspondence should be addressed to Arūnas Tamaševičius; arunas.tamasevicius@ftmc.lt

Received 19 May 2017; Revised 24 July 2017; Accepted 3 August 2017; Published 5 September 2017

Academic Editor: Viet-Thanh Pham

We suggest employing the first-order stable RC filters, based on a single capacitor, for control of unstable fixed points in an array of oscillators. A single capacitor is sufficient to stabilize an entire array, if the oscillators are coupled strongly enough. An array, composed of 24 to 30 mean-field coupled FitzHugh–Nagumo (FHN) type asymmetric oscillators, is considered as a case study. The investigation has been performed using analytical, numerical, and experimental methods. The analytical study is based on the mean-field approach, characteristic equation for finding the eigenvalue spectrum, and the Routh–Hurwitz stability criteria using low-rank Hurwitz matrix to calculate the threshold value of the coupling coefficient. Experiments have been performed with a hardware electronic analog, imitating dynamical behavior of an array of the FHN oscillators.

1. Introduction

A large number of adaptive control techniques have been developed so far to stabilize unstable fixed points (UFP) of dynamical systems. These include derivative control [1–3], tracking filter technique, based on either low-pass or high-pass first-order RC filters [4–9], and notch filter technique that employs two second-order Wien-bridge filters with the incommensurate resonance frequencies [10]. The delayed feedback technique, though originally designed to control chaos, that is, to stabilize unstable periodic orbits [11, 12], under appropriate setting of parameters can stabilize the UFP as well [5, 6, 13–19].

The above-mentioned techniques can stabilize unstable nodes (UFP with even number of real positive eigenvalues λ_i, e.g., $\lambda_{1,2} > 0$ and no imaginary parts of the eigenvalues, i.e., $\mathrm{Im}\,\lambda_{1,2} = 0$) and unstable spirals (UFP with even number of complex eigenvalues with positive real parts, e.g., $\mathrm{Re}\,\lambda_{1,2} > 0$). However, the methods fail to stabilize saddle-type UFP, more specifically, UFP with an odd number of real positive eigenvalues, for example, $\lambda_1 > 0$, $\lambda_2 < 0$. To solve the problem of the odd number limitation, Pyragas and coauthors proposed to use an unstable first-order filter [20, 21]. It was an elegant idea to fight one instability by means of another instability. The method was demonstrated for a variety of mathematical models and experimental systems [20–23]. Later an unstable filter control was developed to stabilize saddle-type UFP in conservative and weakly damped systems [24–26] also under the influence of delay (inertia) in the feedback loop of the controller.

The first-order RC filters, based on a single capacitor, as well as other methods developed for stabilizing the UFP have been applied to single oscillators only. The question thus arises: can a single capacitor stabilize a network of oscillators? The answer depends on the properties of the network. Evidently, if the oscillators in the array are uncoupled or weakly coupled, a single capacitor is insufficient to control the entire network. Each individual oscillator should be provided with a separate controller. Such solution is impractical for applications. However, when the oscillators are coupled strongly enough, one could expect that it is possible to stabilize the entire network using a single controller.

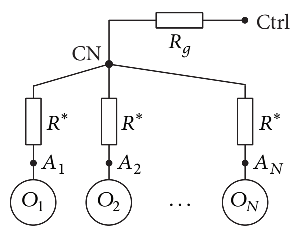

Figure 1: Network of mean-field coupled oscillators, $O_1, O_2, \ldots, O_N$. $A_1, A_2, \ldots, A_N$ are the outputs of the corresponding oscillators and R^* are the coupling resistors. The CN is the coupling node, in general not accessible directly from outside, but via some passive resistive network, represented here by an effective buffer resistor R_g. The Ctrl is an accessible control node.

In this paper, we demonstrate the possibility of stabilizing the network analytically, numerically, and experimentally.

2. Mathematical Model and Its Analysis

To be specific we consider an array of FitzHugh–Nagumo (FHN) oscillators [27], also known in literature as Bonhoeffer–van der Pol (BVP) oscillators [28, 29]. The FHN (or BVP) oscillator actually is a simplified version of the Hodgkin–Huxley (HH) oscillator, imitating the dynamics of spiking neurons [30]. A set of the FHN oscillators is described by

$$\begin{aligned} \dot{x}_i &= ax_i - f(x_i) - y_i - c_i, \\ \dot{y}_i &= x_i - by_i, \quad i = 1, 2, \ldots, N. \end{aligned} \tag{1}$$

Here $f(x_i)$ is a nonlinear function approximated by a three-segment piecewise linear function [31]

$$f(x_i) = \begin{cases} d(x_i + 1), & x_i < -1, \\ 0, & -1 \le x_i \le 1, \\ g(x_i - 1), & x_i > 1. \end{cases} \tag{2}$$

In (2) $d \gg g$. Therefore, $f(x)$ is an essentially asymmetric function, in contrast to common FHN or BVP cubic function x^3 [27–29]. The bias parameters c_i in (1) are intentionally set to be different for each individual oscillator thus making them nonidentical units.

An array of mean-field coupled (star coupling) oscillators is sketched in Figure 1.

The array in Figure 1 is given by the $2N$-dimensional system

$$\begin{aligned} \dot{x}_i &= ax_i - f(x_i) - y_i - c_i + k(\langle x \rangle - x_i), \\ \dot{y}_i &= x_i - by_i, \quad i = 1, 2, \ldots, N. \end{aligned} \tag{3}$$

Here $\langle x \rangle$ is the mean value of the variables x_i

$$\langle x \rangle = \frac{1}{N} \sum_{i=1}^{N} x_i. \tag{4}$$

When an RC tracking filter is applied to the Ctrl node (Figure 1) of the network the overall system becomes $(2N+1)$-dimensional system

$$\begin{aligned} \dot{x}_i &= ax_i - f(x_i) - y_i - c_i + k(z - x_i), \\ \dot{y}_i &= x_i - by_i, \quad i = 1, 2, \ldots, N, \\ \dot{z} &= \omega_f(\langle x \rangle - z). \end{aligned} \tag{5}$$

The cut-off frequency ω_f of the filter should be low ($\omega_f \ll 1$) to ensure tracking the state of the system under control. Note that, in comparison with (3), here in the first equation the mean $\langle x \rangle$ is replaced with its filtered variable z. The case of a single oscillator ($N = 1$, yielding the 3-dimensional system) has been investigated in [31] Analysis of $2N$-dimensional system (3) and $(2N + 1)$-dimensional systems (5) is very complicated. Therefore, we consider a mean-field approach. The mean-field variables are obtained by directly averaging the variables x_i and y_i and the parameters c_i over all oscillators i in (3) and (5), respectively:

$$\begin{aligned} \langle \dot{x} \rangle &= a\langle x \rangle - \langle f(x_i) \rangle - \langle y \rangle - \langle c \rangle, \\ \langle \dot{y} \rangle &= \langle x \rangle - b\langle y \rangle. \end{aligned} \tag{6a}$$

$$\begin{aligned} \langle \dot{x} \rangle &= a\langle x \rangle - \langle f(x_i) \rangle - \langle y \rangle - \langle c \rangle + k(z - \langle x \rangle), \\ \langle \dot{y} \rangle &= \langle x \rangle - b\langle y \rangle, \\ \dot{z} &= \omega_f(\langle x \rangle - z). \end{aligned} \tag{7a}$$

Note that (6a) lacks the term $k(\cdots)$, since $(\langle x \rangle - \langle x \rangle) = 0$.

For $ab < 1$ and $|c| < 1/(b-a)$ the steady-state solutions of (1), (6a), and (7a) are presented by the following fixed points:

$$\begin{aligned} x_{0i} &= -\frac{bc_i}{1 - ab}, \\ y_{0i} &= -\frac{c_i}{1 - ab}, \\ & i = 1, 2, \ldots, N \end{aligned} \tag{8}$$

$$\begin{aligned} \langle x \rangle_0 &= -\frac{b\langle c \rangle}{1 - ab}, \\ \langle y \rangle_0 &= -\frac{\langle c \rangle}{1 - ab}. \end{aligned} \tag{9}$$

$$\begin{aligned} \langle x \rangle_0 &= -\frac{b\langle c \rangle}{1 - ab}, \\ \langle y \rangle_0 &= -\frac{\langle c \rangle}{1 - ab}, \\ z_0 &= -\frac{b\langle c \rangle}{1 - ab}. \end{aligned} \tag{10}$$

Note that the RC tracking filter in (7a) does not change the position of the fixed point: compare (10) with (9). The values given by (10) are independent on k, since $\langle x \rangle_0 = z_0$ and the

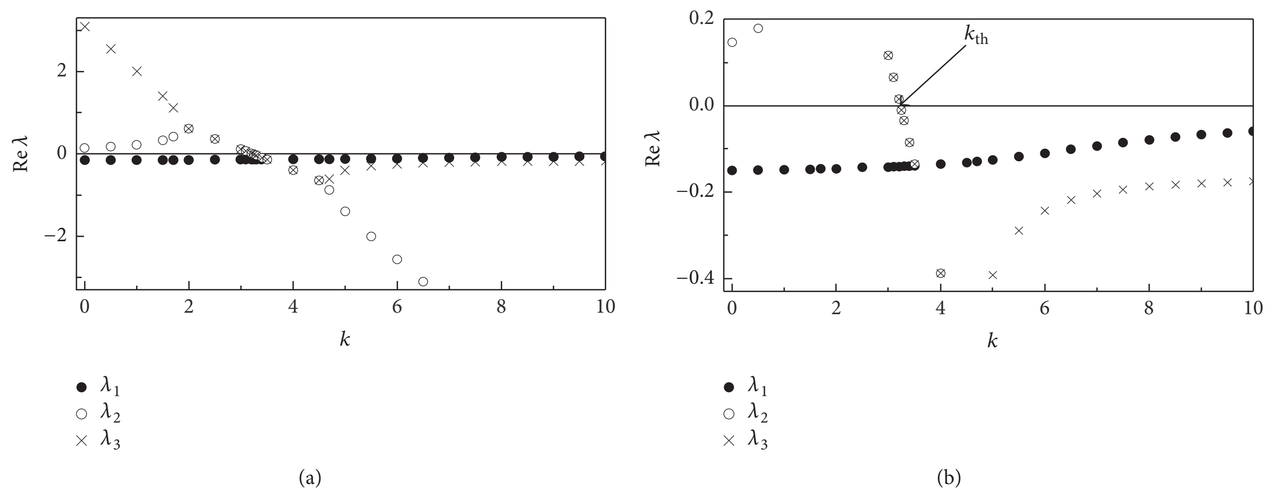

Figure 2: Real parts of the eigenvalues, Re $\lambda_{1,2,3}$ as functions of the coupling parameter k. (a) Full view and (b) vertically stretched view. $a = 3.4$, $b = 0.16$, and $\omega_f = 0.15$. The arrow in plot (b) indicates the coupling parameter $k_{th} = 3.23$, where the largest eigenvalues Re $\lambda_{2,3}$ cross zero axis.

coupling term $k(z - \langle x \rangle)$ in (7a) vanishes for the fixed point. The fixed points (9) and (10) are similar in form to fixed points of the individual uncoupled oscillators (8), except the fact that the fixed points (9) and (10) are single points, whereas (8) yields N points in the phase space.

System (7a), when linearized around the fixed point (10), reads

$$\begin{aligned} \langle \dot{x} \rangle &= a \langle x \rangle - \langle y \rangle + k (z - \langle x \rangle), \\ \langle \dot{y} \rangle &= \langle x \rangle - b \langle y \rangle, \\ \dot{z} &= \omega_f (\langle x \rangle - z). \end{aligned} \tag{11}$$

The corresponding characteristic equation, obtained from differential equation (11) using a standard procedure, has the following algebraic form:

$$\lambda^3 + h_2 \lambda^2 + h_1 \lambda + h_0 = 0, \tag{12}$$

where $h_2 = -a + b + k + \omega_f$, $h_1 = 1 - ab + bk - (a - b)\omega_f$, $h_0 = (1 - ab)\omega_f$.

The fixed point of the mean field is stable, if the real parts of all three eigenvalues Re $\lambda_{1,2,3}$ are negative. Equation (12) has been solved numerically for different values of coupling coefficient k (Figure 2) and the threshold value k_{th}, for which the largest Re $\lambda_{max} = 0$, is found.

In addition, the necessary and sufficient conditions of stability can be estimated analytically from the Hurwitz matrix

$$H = \begin{pmatrix} h_2 & h_0 & 0 \\ 1 & h_1 & 0 \\ 0 & h_2 & h_0 \end{pmatrix}. \tag{13}$$

According to the Routh–Hurwitz stability criterion Re $\lambda_{1,2,3} < 0$ if all diagonal minors of the H-matrix are positive

$$\begin{aligned} \Delta_1 &= h_2 > 0, \\ \Delta_2 &= h_2 h_1 - h_0 > 0, \\ \Delta_3 &= h_0 \Delta_2 > 0. \end{aligned} \tag{14}$$

We start the analysis with Δ_3. Since Δ_2 should be positive according to the second inequality, the third inequality for Δ_3 can be simplified to $h_0 > 0$. This can be further simplified to $ab < 1$, because $\omega_f > 0$ by definition. The inequality $ab < 1$ is always satisfied, since it was used to derive the fixed points (8)–(10). Consequently, we are left with the first and the second inequalities in (14). We define the threshold k_{th} requiring that for $k > k_{th}$ the both minors, Δ_1 and Δ_2 are positive. The first minor $\Delta_1 = h_2$ is rather simple and k_{th1} is readily obtained:

$$k_{th1} = a - b - \omega_f. \tag{15}$$

For the parameter values given in Figure 2, $k_{th1} = 3.09$. The second inequality in (14) is more cumbersome and yields quadratic equation with respect to k_{th2}.

$$p_2 k_{th2}^2 + p_1 k_{th2} + p_0 = 0, \tag{16}$$

where $p_2 = b$, $p_1 = 1 - 2ab + b^2 - (a - 2b)\omega$, $p_0 = -(a - b)[1 - ab - (a - b)\omega + \omega^2]$.

Analytical solution of (16)

$$k_{th} = \frac{\left(-p_1 \pm \sqrt{p_1^2 - 4 p_2 p_0}\right)}{2 p_2} \tag{17}$$

gives two different values: $k'_{th2} = 3.23$ and $k''_{th2} = 0.047$. Finally, we obtain $k_{th} = \max(k_{th1}, k'_{th2}, k''_{th2}) = 3.23$, which is in an excellent agreement with the numerical result, derived from Figure 2(b), where Re $\lambda_{2,3}$ cross the abscissa axis at $k_{th} = 3.23$.

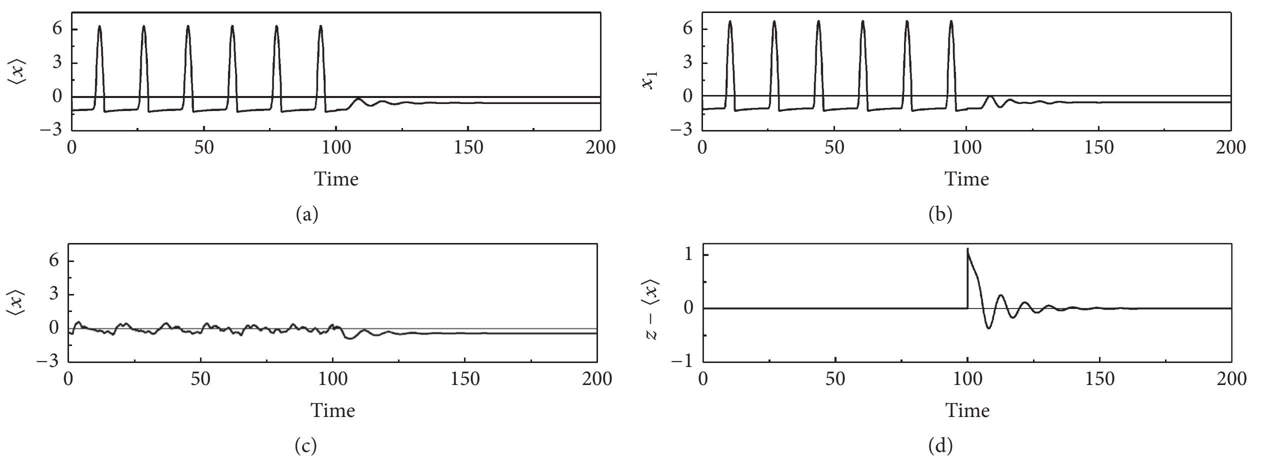

Figure 3: Waveforms from (5). (a) Mean-field variable $\langle x \rangle$ of the synchronized array, (b) dynamical variable x_1 of the first oscillator, (c) mean-field variable $\langle x \rangle$ of the unsynchronized (uncoupled) array, and (d) control term $z - \langle x \rangle$. $N = 24$, $k = 3.4$, $a = 3.4$, $b = 0.16$, and $c_i = 43.5/(24 + i)$, where $i = 1, 2, \ldots, N$, $d = 60$, $g = 3.4$, and $\omega_f = 0.15$. Control is switched on at $t = 100$; in (a), (b), and (d) $\langle x \rangle$ in the coupling term is replaced with z; in (c) the whole control term $k(z - x_i)$ is applied.

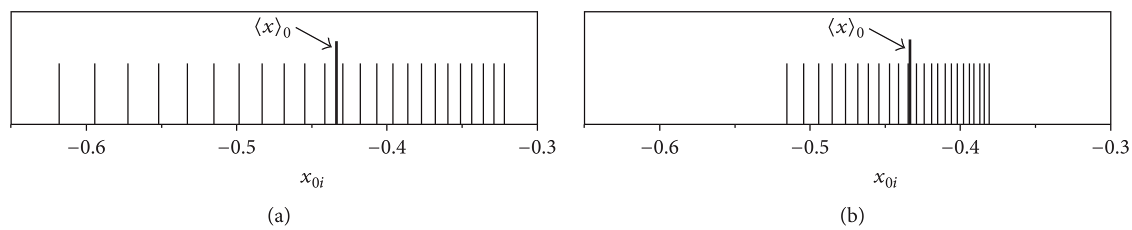

Figure 4: Fixed point spectra x_{0i} ($i = 1, 2, \ldots, 24$). (a) Unsynchronized (uncoupled) oscillators from (8) and (b) stabilized oscillators from numerical solution of (5) at $t = 200$. Parameters are the same as in the caption of Figure 3. The higher and thicker lines in the spectra indicate the mean-field fixed points $\langle x \rangle_0$.

3. Numerical Results

System (5) have been solved numerically using Mathematica, version 9.0 software package. The results are presented in Figure 3. The waveforms of the mean variable $\langle x \rangle(t)$ (Figure 3(a)) and of the individual oscillators, say $x_1(t)$ (Figure 3(b)), look nearly the same, since the array is synchronized. Other variables $x_i(t)$, not shown in Figure 3, have similar form with only small phase shifts, as expected for nonidentical elements. The main difference is in the UFP values x_{0i} due to different bias parameters c_i. The differences between the fixed points x_{0i} of the individual oscillators ($i = 1, 2, \ldots, 24$) are brought out by the fixed point spectra, presented in Figure 4.

It is worth noting that stabilization of the UFP can be achieved in the unsynchronized (uncoupled) array (Figure 3(c)) applying the whole control term $k(z - x_i)$ in (5) at $t = 100$ with a sufficiently large coefficient $k > k_{\text{th}}$. However, this feature is important from a theoretical point of view only. The term $k(z - x_i)$ in (5) means that it controls every individual oscillator "i." It is easy to do in a mathematical model, but in practical (experimental) situations, it requires direct access to every neuronal oscillator. Moreover, from a practical point of view, especially for a possible application to neuronal systems there is no need to stabilize the UFP, if the oscillators are not synchronized. Unsynchronized oscillators yield low mean field, as evidenced by the left hand part ($0 < t < 100$) of the plot in Figure 3(c). For larger arrays, say $N > 100$, the mean field becomes even lower. We recall that in this paper we consider the case of coupled and synchronized oscillators.

In Figure 4(a), $\langle x \rangle_0 = -0.434$ is in a good agreement with the value calculated from (9). In the case of coupled and stabilized array (Figure 3(b)) the spectrum is narrower in comparison with the case of uncoupled oscillators due to strong interaction between oscillators. In Figures 3(a), 3(c), and 4(b)$\langle x \rangle_0 = -0.434$. It well coincides with the value of $\langle x \rangle_0$ in Figure 4(a).

4. Experimental Setup

The experiments have been carried out using an electronic analog array, composed of 30 mean-field coupled FHN type oscillators and described in detail elsewhere [32]. This electronic array has been employed earlier to implement experimentally both the repulsive synchronization [33, 34] and the mean-field nullifying techniques [34, 35].

An individual FHN type oscillator is presented in Figure 5(a). Dimensionless variables x, y, z, and t, as well as the parameters a, b, c, d, g, and k introduced in (5), are related

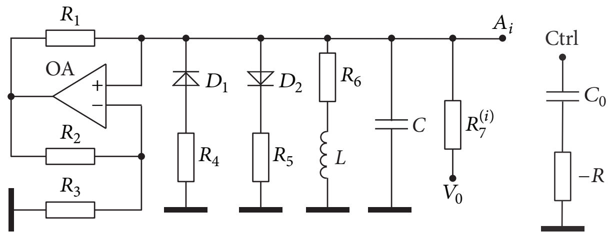

FIGURE 5: Circuit diagrams. (a) FHN asymmetric electronic oscillator. OA is an operational amplifier, for example, NE5534, D_1 and D_2 are the BAV99 type diodes, $V_D = 0.6$ V. $L = 10$ mH, $C = 3.3$ nF, $R_1 = R_2 = 1\,\text{k}\Omega$, $R_3 = 510\,\Omega$, $R_4 = 30\,\Omega$, $R_5 = 510\,\Omega$ ($R_4 \ll R_5$), $R_6 = 275\,\Omega$ (external resistor $220\,\Omega$ in series with the coil ohmic resistance $55\,\Omega$), $R_7 = (24 + i)\,\text{k}\Omega$, $i = 1, 2, \ldots, 30$, and $V_0 = -15$ V. (b) The first-order RC chain. Note the negative resistor "$-R$," used to compensate the positive buffer resistor R_g of the network (see Figure 1). The value of the capacitor C_0 is specified in the caption to Figure 7.

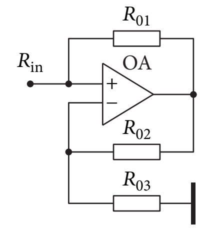

FIGURE 6: Negative impedance converter: active circuit implementation of the negative resistor "$-R$" in Figure 5(b). OA is an operational amplifier, for example, NE5534. $R_{01} = R_{02} = 300\,\Omega$. For $R_{01} = R_{02}$, $R_{\text{in}} = -R_{03}$. The value of the resistor R_{03} is specified in the caption to Figure 7.

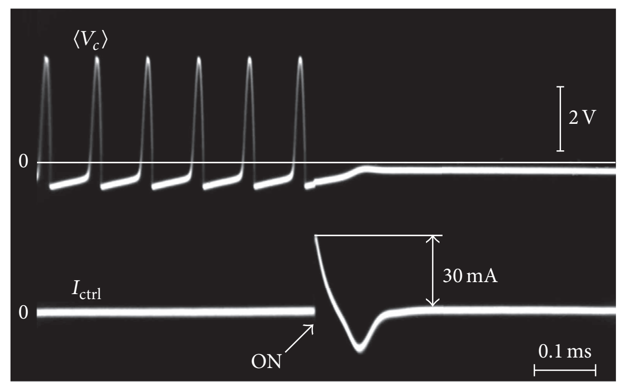

FIGURE 7: Experimental waveforms, the mean-field voltage $\langle V_C \rangle$, and the control current I_{ctrl}. The arrow indicates the time moment, when the RC chain (node Ctrl in Figure 5(b)) is connected to the node Ctrl in Figure 1 (the electronic switch, connecting the controller to the array and its driver is not shown in Figures 1 and 5 for simplicity). $N = 30$, $R^* = 510\,\Omega$, $R_g = 100\,\Omega$, and $R_{03} = 100\,\Omega$ ($R_{\text{in}} = -100\,\Omega$; $R_g + R_{\text{in}} = 0$). $C_0 = 2.2\,\mu$F.

to the electrical values of the analog circuits (Figure 5) in the following way:

$$
\begin{aligned}
x_i &= \frac{V_C^{(i)}}{V_D}, \\
y_i &= \frac{\rho I_L^{(i)}}{V_D}, \\
z &= \frac{V_{C0}}{V_D}, \\
t &\longrightarrow \frac{t}{\sqrt{LC}}, \\
\rho &= \sqrt{\frac{L}{C}}, \\
\omega_f &= \frac{N\sqrt{LC}}{R^* C_0}, \\
a &= \frac{\rho}{R_3}, \\
b &= \frac{R_6}{\rho}, \\
c_i &= \frac{\rho V_0}{R_7^{(i)} V_D}, \\
d &= \frac{\rho}{R_4}, \\
g &= \frac{\rho}{R_5}, \\
k &= \frac{\rho}{R^*}.
\end{aligned}
\tag{18}
$$

Here V_D is the breakpoint voltage of the forward current-voltage characteristic of the diodes.

The negative resistor "$-R$" in Figure 5(b) has been implemented by means of the negative impedance converter (Figure 6) [36]. The input resistance of the NIC $R_{\text{in}} < 0$. The capacitor C_0 with negative resistor "$-R$" in series should not be confused with an unstable RC filter, employed to stabilize saddle-type UFP [25, 26]. Here "$-R$" simply compensates the positive buffer resistor R_g of the network. The RC tracking filters are actually composed of the coupling resistors R^* (Figure 1) and the capacitor C_0; see also definition of the cut-off frequency ω_f in (18).

5. Experimental Results

Experimental waveforms have been taken by means of a digital camera from the screen of a multichannel analog oscilloscope and are shown in Figure 7.

Similarly to the numerical results (Figure 3) the experimental waveform in Figure 7 exhibits negative stabilized state (the nonzero value is due to the dc bias V_0 in Figure 5(a)). Whereas the control current I_{ctrl} in Figure 7 becomes vanishingly small after a relatively short transient process.

6. Discussion

The investigation performed here is not an end in itself. The purpose of the study is the search of practical techniques inhibiting activity of neuronal arrays. It is widely believed that strong synchrony of spiking neurons in the brain causes the symptoms of Parkinson's disease [37].

One of the simplest methods to damp spiking neurons is the external stimulation of certain brain areas with strong high frequency (about 100 to 150 Hz) periodic pulses. It is a conventional clinically approved therapy for patients with the Parkinson's symptoms, so-called deep brain stimulation (DBS) [38–40]. Unfortunately, the DBS treatment is often accompanied with undesirable side effects. In recent papers [41–43], it has been demonstrated that the high frequency forcing eventually stabilizes the UFP of the neuronal oscillators in case of HH, FHN, and other neuronal models. Two shortcomings of the DBS have been emphasized [43]. Firstly, though the spiking neurons are suppressed, relatively high amplitude (10 to 20%) high frequency artifact oscillations are observed. Secondly, the fixed points of the membrane voltages are essentially moved from their natural values because of the rectifying effect in the cells [43]. This can be a reason of the side effects.

A number of more sophisticated methods to avoid synchronization of interacting oscillators in general and more specifically with the possible application to neuronal arrays have been described in literature, for example [33, 37, 44–54].

Specifically, in [47] suppression of synchrony of coupled oscillators by means of a passive oscillator is described. The controller is a four-terminal third-order device with separate recording and field application electrodes. The feedback loop contains a second-order damped oscillator, an integrator, an adder, and two amplifiers. Our controller is much simpler. It is a two-terminal first-order device with the same voltage sensing and current application electrode. The controller contains a single capacitor and a negative impedance converter (NIC) based on a single operational amplifier. The NIC is not necessary, if the buffer resistance R_g is small.

In addition, a recently found phenomenon of oscillation quenching in the systems of coupled nonlinear oscillators is worth mentioning [55–58]. It can manifest via two different mechanisms, the so-called oscillation death and amplitude death. The effect, in particular the oscillation death, can be perspective for oscillation suppression in neuronal disorders, such as the Parkinson's disease and essential tremor. This type of oscillation quenching depends on the intrinsic parameters of the individual oscillators, but even more on the way and the strength of coupling. The parameters of the oscillators and the parameters of coupling can be easily controlled in the artificially made physical, chemical, electronic, and so on systems. However, these parameters are difficult to tune in natural, for example, biological, systems. Therefore, the techniques employing external feedback loops seem to be advantageous solutions.

7. Conclusions

An array of coupled neuronal type oscillators, specifically the FitzHugh–Nagumo cells, can be stabilized by means of a single capacitor based RC filter feedback technique. The feedback signals become vanishingly small, when the UFP is stabilized, similarly to the feedback suppression of synchrony described in [47]. This can be an advantage over the nonfeedback techniques, for example, the DBS employing external high frequency periodic forcing.

Our future work will focus on the investigation of an array of weakly coupled FHN oscillators ($k < k_{th}$), when stabilization of the UFP is impossible. We hope that a single capacitor based RC filter can desynchronize oscillators in the array, somewhat likewise to the repulsive coupling [33, 34] and the mean-field nullifying [34, 35] techniques.

Conflicts of Interest

The authors declare that there are no conflicts of interest regarding the publication of this paper.

Acknowledgments

The authors thank Dr. Nikolai Rulkov for critical discussion of the results and especially for the suggestion of emphasizing the effect of control at the level of individual elements and also for drawing their attention to the fact that there is no reason for the array, given by (5), to oscillate synchronously before the control term is applied. The authors are also grateful to Professor Michael Rosenblum for drawing their attention to the fact that, in paper [47], along with the suppression of synchrony in an ensemble of interacting units, stabilization of an active oscillator by means of a passive oscillator, included in the feedback loop, is also described.

References

[1] S. Bielawski, M. Bouazaoui, D. Derozier, and P. Glorieux, "Stabilization and characterization of unstable steady states in a laser," *Physical Review A*, vol. 47, no. 4, pp. 3276–3279, 1993.

[2] G. A. Johnston and E. R. Hunt, "Derivative control of the steady state in chua's circuit driven in the chaotic region," *IEEE Transactions on Circuits and Systems I*, vol. 40, no. 11, pp. 833–835, 1993.

[3] P. Parmananda, M. A. Rhode, G. A. Johnson, R. W. Rollins, H. D. Dewald, and A. J. Markworth, "Stabilization of unstable steady states in an electrochemical system using derivative control," *Physical Review E*, vol. 49, no. 6, pp. 5007–5011, 1994.

[4] N. F. Rulkov, L. S. Tsimring, and H. D. I. Abarbanel, "Tracking unstable orbits in chaos using dissipative feedback control," *Physical Review E*, vol. 50, no. 1, pp. 314–324, 1994.

[5] A. Namajūnas, K. Pyragas, and A. Tamaševičius, "Stabilization of an unstable steady state in a Mackey-Glass system," *Physics Letters A*, vol. 204, no. 3-4, pp. 255–262, 1995.

[6] A. Namajūnas, K. Pyragas, and A. Tamaševičius, "Analog techniques for modeling and controlling the Mackey-Glass system," *International Journal of Bifurcation and Chaos in Applied Sciences and Engineering*, vol. 7, no. 4, pp. 957–962, 1997.

[7] M. Ciofini, A. Labate, R. Meucci, and M. Galanti, "Stabilization of unstable fixed points in the dynamics of a laser with feedback," *Physical Review E*, vol. 60, no. 1, pp. 398–402, 1999.

[8] A. S. Zu Schweinsberg and U. Dressler, "Characterization and stabilization of the unstable fixed points of a frequency doubled

Nd: YAG laser," *Physical Review E*, vol. 63, no. 5, pp. 562101–5621012, 2001.

[9] H. Huijberts, "Linear controllers for the stabilization of unknown steady states of chaotic systems," *IEEE Transactions on Circuits and Systems. I. Regular Papers*, vol. 53, no. 10, pp. 2246–2254, 2006.

[10] A. Ahlborn and U. Parlitz, "Chaos control using notch filter feedback," *Physical Review Letters*, vol. 96, no. 3, article 034102, 2006.

[11] K. Pyragas, "Continuous control of chaos by self-controlling feedback," *Physics Letters A*, vol. 170, no. 6, pp. 421–428, 1992.

[12] K. Pyragas and A. Tamaševičius, "Experimental control of chaos by delayed self-controlling feedback," *Physics Letters A*, vol. 180, no. 1-2, pp. 99–102, 1993.

[13] K. Pyragas, "Control of chaos via extended delay feedback," *Physics Letters. A*, vol. 206, no. 5-6, pp. 323–330, 1995.

[14] A. Chang, J. C. Bienfang, G. M. Hall, J. R. Gardner, and D. J. Gauthier, "Stabilizing unstable steady states using extended time-delay autosynchronization," *Chaos*, vol. 8, no. 4, pp. 782–790, 1998.

[15] P. Hövel and E. Schöll, "Control of unstable steady states by time-delayed feedback methods," *Physical Review E*, vol. 72, no. 4, article 046203, pp. 23–46, 2005.

[16] S. Yanchuk, M. Wolfrum, P. Hövel, and E. Schöll, "Control of unstable steady states by long delay feedback," *Physical Review E*, vol. 74, no. 2, article 026201, 2006.

[17] Y. Ding, W. Jiang, and H. Wang, "Delayed feedback control and bifurcation analysis of Rossler chaotic system," *Nonlinear Dynamics*, vol. 61, no. 4, pp. 707–715, 2010.

[18] B. Rezaie and M.-R. Jahed Motlagh, "An adaptive delayed feedback control method for stabilizing chaotic time-delayed systems," *Nonlinear Dynamics*, vol. 64, no. 1-2, pp. 167–176, 2011.

[19] A. Gjurchinovski, T. Jüngling, V. Urumov, and E. Schöll, "Delayed feedback control of unstable steady states with high-frequency modulation of the delay," *Physical Review E*, vol. 88, no. 3, article 032912, 2013.

[20] K. Pyragas, V. Pyragas, I. Z. Kiss, and J. L. Hudson, "Stabilizing and tracking unknown steady states of dynamical systems," *Physical Review Letters*, vol. 89, no. 24, pp. 2441031–2441034, 2002.

[21] K. Pyragas, V. Pyragas, I. Z. Kiss, and J. L. Hudson, "Adaptive control of unknown unstable steady states of dynamical systems," *Physical Review E*, vol. 70, no. 2, article 026215, 2004.

[22] D. J. Braun, "Adaptive steady-state stabilization for nonlinear dynamical systems," *Physical Review E*, vol. 78, no. 1, article 016213, 2008.

[23] A. Tamaševičius, E. Tamaševičiute, G. Mykolaitis, and S. Bumelienė, "Switching from stable to unknown unstable steady states of dynamical systems," *Physical Review E*, vol. 78, no. 2, article 026205, 2008.

[24] A. Tamaševičius, E. Tamaševičiūtė, G. Mykolaitis, S. Bumelienė, and R. Kirvaitis, "Stabilization of saddle steady states of conservative and weakly damped dissipative dynamical systems," *Physical Review E*, vol. 82, no. 2, article 026205, 2010.

[25] A. Tamaševičius, E. Tamaševičiute, G. Mykolaitis, and S. Bumelienė, "Enhanced control of saddle steady states of dynamical systems," *Physical Review E*, vol. 88, no. 3, article 032904, 2013.

[26] E. Tamaševičiūtė, G. Mykolaitis, S. Bumelienė, and A. Tamaševičius, "Stabilizing saddles," *Physical Review E*, vol. 88, no. 6, article 060901 (R), 2013.

[27] R. Fitzhugh, "Impulses and physiological states in theoretical models," *Biophysical Journal*, vol. 1, no. 6, pp. 445–466, 1961.

[28] A. Rabinovitch, R. Thieberger, and M. Friedman, "Forced Bonhoeffer-van der Pol oscillator in its excited mode," *Physical Review E*, vol. 50, no. 2, pp. 1572–1578, 1994.

[29] M. Sekikawa, K. Shimizu, N. Inaba et al., "Sudden change from chaos to oscillation death in the Bonhoeffer-van der Pol oscillator under weak periodic perturbation," *Physical Review E*, vol. 84, no. 5, article 056209, 2011.

[30] W. Gerstner and W. M. Kistler, *Spiking Neuron Models: Single Neurons, Populations, Plasticity*, Cambridge University Press, Cambridge, UK, 2002.

[31] A. Tamaševičius, E. Tamaševičiute, G. Mykolaitis, S. Bumelienė, R. Kirvaitis, and R. Stoop, "Neural spike suppression by adaptive control of an unknown steady state," *Lecture Notes in Computer Science*, vol. 5768, no. 1, pp. 618–627, 2009.

[32] E. Tamaševičiūtė, G. Mykolaitis, and A. Tamaševičius, "Analogue modelling an array of the FitzHugh-Nagumo oscillators," *Nonlinear Analysis: Modelling and Control*, vol. 17, no. 1, pp. 118–125, 2012.

[33] L. S. Tsimring, N. F. Rulkov, M. L. Larsen, and M. Gabbay, "Repulsive synchronization in an array of phase oscillators," *Physical Review Letters*, vol. 95, no. 1, article 014101, 2005.

[34] A. Tamaševičius, E. Tamaševičiute, and G. Mykolaitis, "Feedback controller for destroying synchrony in an array of the FitzHugh-Nagumo oscillators," *Applied Physics Letters*, vol. 101, no. 22, article 223703, 2012.

[35] A. Tamaševičius, G. Mykolaitis, E. Tamaševičiūtė, and S. Bumelienė, "Two-terminal feedback circuit for suppressing synchrony of the Fitz Hugh–Nagumo oscillators," *Nonlinear Dynamics*, vol. 81, no. 1-2, pp. 783–788, 2015.

[36] P. Horowitz and W. Hill, *The Art of Electronics*, Cambridge University Press, Cambridge, UK, 1993.

[37] M. G. Rosenblum and A. S. Pikovsky, "Controlling synchronization in an ensemble of globally coupled oscillators," *Physical Review Letters*, vol. 92, article 114102, 2004.

[38] S. Breit, J. B. Schulz, and A.-L. Benabid, "Deep brain stimulation," *Cell and Tissue Research*, vol. 318, no. 1, pp. 275–288, 2004.

[39] J. S. Perlmutter and J. W. Mink, "Deep brain stimulation," *Annual Review of Neuroscience*, vol. 29, pp. 229–257, 2006.

[40] A. L. Benabid, S. Chabardes, J. Mitrofanis, and P. Pollak, "Deep brain stimulation of the subthalamic nucleus for the treatment of Parkinson's disease," *The Lancet Neurology*, vol. 8, no. 1, pp. 67–81, 2009.

[41] K. Pyragas, V. Novičenko, and P. A. Tass, "Mechanism of suppression of sustained neuronal spiking under high-frequency stimulation," *Biological Cybernetics*, vol. 107, no. 6, pp. 669–684, 2013.

[42] K. Pyragas and P. A. Tass, "Suppression of spontaneous oscillations in high-frequency stimulated neuron models," *Lithuanian Journal of Physics*, vol. 56, no. 4, pp. 223–238, 2016.

[43] E. Adomaitienė, G. Mykolaitis, S. Bumelienė, and A. Tamaševičius, "Inhibition of spikes in an array of coupled FitzHugh–Nagumo oscillators by external periodic forcing," *Nonlinear Analysis: Modelling and Control*, vol. 22, no. 3, pp. 421–429, 2017.

[44] O. V. Popovych, C. Hauptmann, and P. A. Tass, "Effective desynchronization by nonlinear delayed feedback," *Physical Review Letters*, vol. 94, no. 16, article 164102, 2005.

[45] O. V. Popovych, C. Hauptmann, and P. A. Tass, "Control of neuronal synchrony by nonlinear delayed feedback," *Biological Cybernetics*, vol. 95, no. 1, pp. 69–85, 2006.

[46] P. A. Tass, *Phase Resetting in Medicine and Biology: Stochastic Modelling and Data Analysis*, Springer, Berlin, Germany, 2007.

[47] N. Tukhlina, M. Rosenblum, A. Pikovsky, and J. Kurths, "Feedback suppression of neural synchrony by vanishing stimulation," *Physical Review E*, vol. 75, no. 1, article 011918, 2007.

[48] K. Pyragas, O. V. Popovych, and P. A. Tass, "Controlling synchrony in oscillatory networks with a separate stimulation-registration setup," *Europhysics Letters*, vol. 80, no. 4, article 40002, 2007.

[49] M. Luo and J. Xu, "Suppression of collective synchronization in a system of neural groups with washout-filter-aided feedback," *Neural Networks*, vol. 24, no. 6, pp. 538–543, 2011.

[50] H. Hong and S. H. Strogatz, "Kuramoto model of coupled oscillators with positive and negative coupling parameters: an example of conformist and contrarian oscillators," *Physical Review Letters*, vol. 106, no. 5, article 054102, 2011.

[51] A. Franci, A. Chaillet, E. Panteley, and F. Lamnabhi-Lagarrigue, "Desynchronization and inhibition of Kuramoto oscillators by scalar mean-field feedback," *Mathematics of Control, Signals, and Systems*, vol. 24, no. 1-2, pp. 169–217, 2012.

[52] G. Montaseri, M. J. Yazdanpanah, A. Pikovsky, and M. Rosenblum, "Synchrony suppression in ensembles of coupled oscillators via adaptive vanishing feedback," *Chaos*, vol. 23, no. 3, article 033122, 2013.

[53] I. Ratas and K. Pyragas, "Controlling synchrony in oscillatory networks via an act-and-wait algorithm," *Physical Review E*, vol. 90, no. 3, article 032914, 2014.

[54] I. Ratas and K. Pyragas, "Eliminating synchronization in bistable networks," *Nonlinear Dynamics*, vol. 83, no. 3, pp. 1137–1151, 2016.

[55] A. Koseska, E. Volkov, and J. Kurths, "Transition from amplitude to oscillation death via turing bifurcation," *Physical Review Letters*, vol. 111, no. 2, article 024103, 2013.

[56] A. Koseska, E. Volkov, and J. Kurths, "Oscillation quenching mechanisms: amplitude vs. oscillation death," *Physics Reports*, vol. 531, no. 4, pp. 173–199, 2013.

[57] W. Zou, D. V. Senthilkumar, A. Koseska, and J. Kurths, "Generalizing the transition from amplitude to oscillation death in coupled oscillators," *Physical Review E*, vol. 88, no. 5, article 050901, 2013.

[58] A. Gjurchinovski, A. Zakharova, and E. Schöll, "Amplitude death in oscillator networks with variable-delay coupling," *Physical Review E*, vol. 89, no. 3, article 032915, 2014.